Clim. Past, 18, 1529–1539, 2022
https://doi.org/10.5194/cp-18-1529-2022
© Author(s) 2022. This work is distributed under
the Creative Commons Attribution 4.0 License.

Climate of the Past
Open Access

Development of longitudinal dunes under Pangaean atmospheric circulation

Hiroki Shozaki[1,★] **and Hitoshi Hasegawa**[2,★]

[1]Earth-Life Science Institute, Tokyo Institute of Technology, Tokyo, 152-8550, Japan
[2]Department of Global Environment and Disaster Prevention, Faculty of Science and Technology, Kochi University, Kochi 780-8520, Japan
★These authors contributed equally to this work.

Correspondence: Hiroki Shozaki (hi.shozaki@elsi.jp) and Hitoshi Hasegawa (hito_hase@kochi-u.ac.jp)

Received: 10 December 2021 – Discussion started: 20 December 2021
Revised: 9 June 2022 – Accepted: 10 June 2022 – Published: 5 July 2022

Abstract. As a result of the large difference in heat capacity between land and ocean, global climate and atmospheric circulation patterns over the supercontinent of Pangaea were significantly different from those of today. Modelling experiments indicate a seasonal alternation in cross-equatorial flow induced by the seasonal reversal in the direction of the monsoonal circulation; however, there are large discrepancies between model-generated surface wind patterns and the reported palaeowind directions from aeolian dune records. Here, we present the spatial distribution of dune slip-face azimuths recorded in the Lower Jurassic aeolian sandstones over a wide area of the western United States (palaeolatitude: ∼ 19–27° N). The azimuth data for dune slip faces reveal a bidirectional and oblique angular pattern that resembles the internal structures of modern longitudinal dunes. Based on the spatial pattern of slip-face directions and outcrop evidence, we suggest that most Lower Jurassic aeolian sandstones were NNE–SSW- to NNW–SSE-oriented longitudinal dunes, which likely formed as the result of a combination of westerly, northwesterly, and northeasterly palaeowinds. The reconstructed palaeowind pattern at ∼ 19–27° N appears to be consistent with the model-generated surface wind pattern and its seasonal alternation. The reconstructed palaeowind patterns also suggest an influence of orbitally induced changes in atmospheric pressure patterns over Pangaea.

1 Introduction

From the Carboniferous to the Jurassic, the supercontinent Pangaea dominated Earth. Because Pangaea was the largest pole-to-pole landmass in Earth's history, atmospheric circulation during this period is thought to have differed substantially from that of today (Kutzbach and Gallimore, 1989; Parrish, 1993). Modelling experiments have indicated that Pangaean atmospheric circulation was characterized by cross-equatorial wind flow induced by strong monsoonal circulation and large seasonal movement of the intertropical convergence zone (ITCZ) to near to 30° on land in both hemispheres (Kutzbach and Gallimore, 1989; Parrish, 1993; Rowe et al., 2007). Some studies have also suggested significant changes in atmospheric pressure patterns over Pangaea caused by orbital-scale changes in the seasonal and latitudinal distributions of solar radiation (Kutzbach, 1994; Winguth and Winguth, 2013). However, the terrestrial environmental response to such seasonal- and orbital-scale changes in atmospheric pressure patterns during this period remains poorly known.

The aeolian dune record provides information on the prevailing surface wind regime and atmospheric circulation patterns in the past (Lancaster, 1981, 1990; Parrish and Peterson, 1988; Peterson, 1988; Livingstone, 1989; Kocurek, 1991; Scherer, 2000; Lancaster et al., 2002; Loope et al., 2004; Beveridge et al., 2006; Sridhar et al., 2006; Rodríguez-López et al., 2008; Hasegawa et al., 2012). Modern deserts mostly develop in the subtropical high-pressure belt as a result of downwelling of the Hadley circulation, except for the interiors of Eurasia and North America, where a continental climate and monsoonal circulation are predominant. Aeolian dunes in desert areas record the prevailing surface wind pattern (e.g. trade winds and westerlies) in the form of large-scale cross-beds (Breed et al., 1979; Lancaster, 1981; Wasson et al., 1988; Hesse, 2010; Hasegawa et al., 2012). In addition, patterns of dune alignment and morphology have been considered to reflect the prevailing wind regime and mesoscale circulation patterns along with seasonal and long-term variations in wind direction (Bristow et al., 2000, 2007; Beveridge et al., 2006; Sridhar et al., 2006; Zhou et al., 2012; Telfer and Hesse, 2013; Liu and Baas, 2020), although dune morphology also depends on sediment availability, erodibility, and vegetation cover (du Pont et al., 2014; Gao et al., 2015). The spatial distribution of palaeowind patterns inferred from aeolian dune slip-face azimuths thus allows the deduction of atmospheric circulation patterns in geological periods characterized by different land–sea distributions (Parrish and Peterson, 1988; Peterson, 1988; Scherer, 2000; Loope et al., 2004) or different palaeoclimatic settings (Beveridge et al., 2006; Sridhar et al., 2006; Rodríguez-López et al., 2008; Hasegawa et al., 2012).

Peterson (1988) initially described the spatial and temporal changes in palaeowind regimes from Carboniferous to Middle Jurassic aeolian sandstone in the western United States (US) (i.e. the Colorado Plateau and surrounding area). Using these datasets and published palaeomagnetic data, Loope et al. (2004) suggested the predominance of a desert environment in the Pangaean equatorial area (palaeolatitude 8–13° N), with a broad sweep of SW-ward winds in the northern area changing to SE-ward winds in the southern area during the Early Jurassic. However, the reconstructed surface wind pattern shows discrepancies with the results of model-based reconstructions (Rowe et al., 2007), even though the revised palaeolatitude of the Colorado Plateau (17–24° N) has been used. Rowe et al. (2007) suggested several possible reasons for this discrepancy, including that (1) the palaeomagnetism-based palaeogeographic reconstructions of the Jurassic are incorrect, (2) the interpretation of how winds shaped the dunes is mistaken, or (3) the basic climate controls during the Jurassic were different from those of today.

We considered the problems involved in the measurement of palaeowind direction data from the aeolian dune record. Peterson (1988) provided only single preferred palaeowind directions at each site without information on dune morphology, thus hindering the understanding of accurate palaeowind flow regimes. Therefore, a re-evaluation of the palaeowind direction data with a particular focus on dune morphology and a multi-directional wind regime could explain the discrepancy between reconstructed surface wind patterns and model-based reconstructions. In addition, recent palaeomagnetic studies that addressed the inclination-shallowing problem (Kent and Irving, 2010; Dickinson, 2018) provide the revised palaeolatitude of the Colorado Plateau as 19–27° N during the Early Jurassic, which corresponds to the location of the model-generated desert area and the subtropical high-pressure belt (Rowe et al., 2007). To solve the discrepancies between model experiments and wind patterns inferred from aeolian dune records, a re-evaluation of the Lower Jurassic aeolian dune slip-face azimuth record that considers the latest palaeogeographical reconstruction is required.

Here, we present the spatial distribution of slip-face azimuths and the inferred dune morphology recorded in Lower Jurassic aeolian sandstones in the western US, together with the latest palaeolatitude data (Kent and Irving, 2010; Dickinson, 2018). Our measurement of slip-face orientations over a wide area of the western US and field observational evidence reveal the presence of longitudinal dunes in the Early Jurassic desert that formed as a result of tridirectional palaeowind patterns, consistent with model-generated seasonal wind regimes (Rowe et al., 2007). We also discuss a possible relation between the formation process of longitudinal dunes and orbitally induced changes in the atmospheric pressure pattern by comparing the inferred wind patterns with a climate model reconstruction for the Pangaea supercontinent (Winguth and Winguth, 2013).

2 Material and methods

2.1 Lower Jurassic aeolian sandstone

To obtain the spatial distributions of palaeowind directions, we surveyed Lower Jurassic aeolian sandstone strata and measured the maximum slip-face azimuths of the dunes over a wide area in the western US, specifically the Navajo Sandstone on the Colorado Plateau (Utah, Colorado, and Arizona) and correlative strata of the Nugget Sandstone to the north (Idaho, Wyoming) and the Aztec Sandstone to the south (Nevada) (Fig. 1). The maximum thickness of the strata is ~ 700 m, in southern-central Utah, thinning to ~ 100–150 m in the northern area (Nugget Sandstone in Idaho and Wyoming) and eastern area (Glen Canyon Sandstone in western Utah and Colorado) (Blakey et al., 1988; Parrish and Peterson, 1988; Peterson, 1988; Blakey, 2008). The estimated size of the palaeodune field is $\sim 625\,000$ km^2, which is 2.5 times larger than the size of the remaining outcrop (Marzolf, 1988; Kocurek, 2003; Tape, 2005). On the basis of existing palaeomagnetic studies (Kent and Irving, 2010; Dickinson, 2018), the palaeolatitude of the studied palaeodune field is inferred to have been ca. 19–27° N during the Early Jurassic, with clockwise rotation of the continent by $\sim 5°$.

The chronology and correlation of the Lower Jurassic aeolian sandstone (Navajo Sandstone and correlative strata) in the western US are debated (Dickinson and Gehrels, 2009; Dickinson et al., 2010; Sprinkel et al., 2011; Rowland and Mercadante, 2014; Parrish et al., 2019). Based on U–Pb age dating of detrital zircons, the depositional ages of the underlying Kayenta Formation and overlying Page Sand-

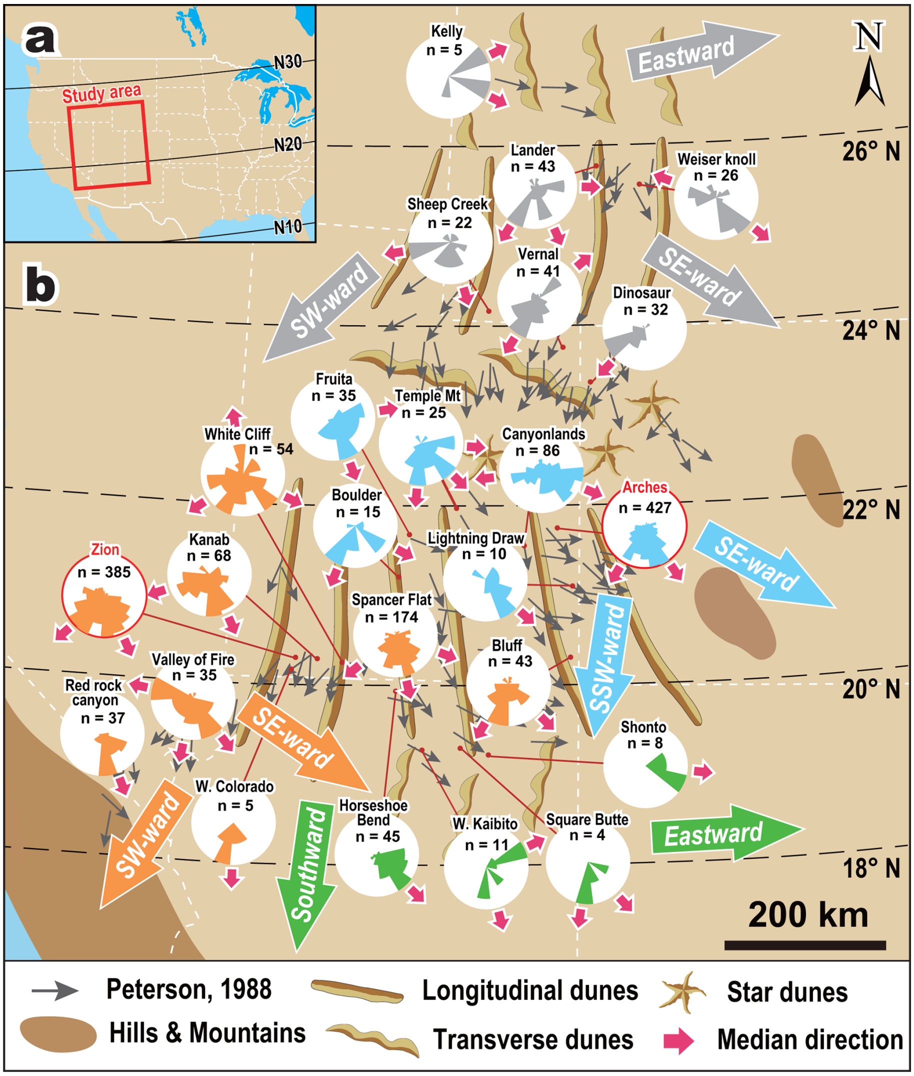

Figure 1. Reconstructed palaeowind patterns in the western US during the Early Jurassic. **(a)** Location of the study area in the western US. **(b)** Spatial distributions of dune slip-face azimuths measured in this study (shown on rose diagrams) and inferred dune morphologies plotted on the Early Jurassic palaeogeographic map of Peterson (1988), with palaeolatitudes based on Dickinson (2018). The colours of the rose diagrams indicate the area: northern (grey), central (light blue), southwestern (orange), and southern (green) parts of the study area. Large arrows in **(b)** indicate the reconstructed prevailing surface wind directions in each area. The pink arrows around the outside of each rose diagram indicate the median directions of separated components in the slip-face azimuth data provided in Table 1.

stone are considered to be 190–187 and 170 ± 3 Ma, respectively (Dickinson and Gehrels, 2009). The U–Pb and $^{40}Ar/^{39}Ar$ ages of pyroclastic zircon and biotite crystals from tephra lenses in the basal part of the Page Sandstone yield an upper age limit for the Navajo Sandstone of 172.3–170.6 Ma (Dickinson et al., 2010). Based on these existing ages, the duration of the deposition of the Lower Jurassic aeolian sandstone is estimated to be ca. 14.7–19.4 Myr. On the other hand, Parrish et al. (2019) proposed a much older age (200.5 ± 1.5 Ma and 195.0 ± 7.7 M) for the Navajo Sandstones in southeastern Utah based on U–Pb analyses of carbonate deposits. These ages suggest that the basal part of the Navajo Sandstone and the underlying Kayenta Formation are interfingered or even time-transgressive over a period of several million years (Parrish et al., 2019).

Stratigraphic correlation of cross-strata in the Lower Jurassic aeolian sandstone over a wide area of western US is challenging due to the chronological problems described above and a lack of first-order bounding surfaces with a wide extent. Although it is difficult to accurately correlate the strata among regions, we investigated the palaeowind records over a wide area to obtain the spatial distribution of palaeowind directions as shown in Fig. 1. The results may not represent truly contemporaneous datasets at different sites, and determining the exact spatial distribution for a given time window needs further chronological research. Nevertheless,

Table 1. Calculated median directions of slip-face azimuths at each site. The original data are provided in the table in the Supplement.

Study site	Number of data	Median direction 1	Median direction 2	Median direction 3	Study site	Number of data	Median direction 1	Median direction 2	Median direction 3
Kelly*	5	63.5°	116.0°	–	Zion	385	156.3°	228.3°	–
Lander*	43	91.0°	156.0°	212.0°	Kanab	68	156.4°	252.1°	–
Weiser Knoll	26	129.7°	290.5°	–	White Cliff	54	116.2°	236.2°	351.7°
Sheep Creek	22	163.8°	260.6°	–	Spencer Flat	174	111.3°	166.6°	230.4°
Vernal	41	49.7°	212.7°	–	Bluff*	43	135.5°	211.0°	–
Dinosaur	32	223.9°	–	–	Red Rock Canyon	37	159.3°	–	–
Fruita	35	81.5°	159.4°	–	Valley of Fire	35	143.3°	192.0°	282.8°
Temple Mountain*	25	94.0°	135.0°	185.0°	Western Colorado City	5	182.0°	–	–
Canyonlands	86	112.3°	264.0°	–	Horseshoe Bend	45	134.6°	–	–
Arches*	427	146.0°	211.0°	–	Western Kaibito	11	64.0°	165.2°	–
Lightning Draw	10	132.0°	–	–	Square Butte	4	137.6°	188.5°	–
Boulder	15	118.3°	202.8°	–	Shonto	8	96.0°	–	–

* The separation of components and median directions at these sites is based on histograms of the slip-face azimuth distribution.

we believe that the spatial distribution of palaeowind directions presented in this study is important because it represents an integrated pattern of mesoscale wind regimes in the western US area of the Pangaea supercontinent during the Early Jurassic.

2.2 Reconstruction of spatial palaeowind patterns

Palaeowind directions at each site were determined based on measurements of the maximum slip-face dip azimuths at each outcrop of cross-bedding strata. In total, we measured 1636 slip-face azimuths from 178 sites (see the table in the Supplement). Unlike Peterson (1988), who reported only single preferred palaeowind directions at each site, we provide the multi-directional palaeowind regime as the rose diagrams shown in Fig. 1. We also show regional-scale slip-face azimuth data and outcrop evidence for the Navajo Sandstone in Zion National Park (southwestern Utah) and Arches National Park (eastern Utah) (Figs. 2 and 3). The slip-face azimuth data were corrected for the magnetic declination (+11°) in the western US (Thébault et al., 2015) and the bedding tilt using the Kyoto Untilting Tool software (Tomita and Yamaji, 2003) developed by the Yamaji Laboratory, Kyoto University. The obtained slip-face azimuth data were then corrected for post-Jurassic clockwise rotation of the continent (5°) and plotted on a palaeogeographic map (Fig. 1) with palaeolatitudes based on palaeomagnetic data (Dickinson, 2018; Kent and Irving, 2010). The palaeowind data were plotted on rose diagrams using the analytical software Rose, developed by the Naruse Laboratory, Kyoto University.

The obtained slip-face azimuth data commonly show multiple palaeowind directions in the rose diagrams. To statistically separate multiple palaeowind directions and calculate the median directions, we used a "Gaussian mixture" (GM) model, assuming that the data distribution reflects a mixture of a finite number of Gaussian (normal) distributions. Using an expectation-maximization (EM) algorithm to fit the GM model, we separated slip-face azimuth data into multiple components (distributions) and finally calculated the median palaeowind directions at each site. The number of components was determined either by cluster analysis or from the number of major peaks in histograms of slip-face azimuth data at each site (Table 1).

3 Results and discussion

3.1 Development of NNE–SSW- to NNW–SSE-oriented longitudinal dunes

The spatial distribution of dune slip-face azimuths obtained in this study indicates multiple directions of palaeowind flow, mainly eastward, southeastward, and southwestward (Fig. 1b). Although Peterson (1988) reported a single preferred palaeowind direction for each region, which is, overall, consistent with our data, the obtained datasets show multiple directions. In addition, the slip-face azimuths in most of the regions show bidirectional and oblique angular variation between ~ 80 and 135°.

Outcrop evidence of slip-face azimuth data of the Navajo Sandstone in Zion National Park and Arches National Park are illustrated in Figs. 2 and 3, respectively. The rose diagrams for the Zion region show bimodal preferred directions toward the SSE and SW (centred at ~ 160 and ~ 240°). In addition, the preferred direction switches between SSE-wards and SW-wards at horizontal intervals of ~ 1 km (Fig. 2a). The rose diagrams of the Arches region also show bimodal preferred directions to the SE and SSW (centred at ~ 140 and ~ 220°) and changes in preferred directions at horizontal intervals of ~ 1–2 km (Fig. 3a). In both regions, the outcrops located at the boundaries between areas of bidirectional and oblique angular slip-face directions show zigzagging patterns and compound sets of cross-stratification (Figs. 2c and 3c). The observed bidirectional cross-bed structures exhibit a marked correspondence with the internal structures of modern longitudinal dunes as reconstructed from ground-penetrating radar (GPR) profiles

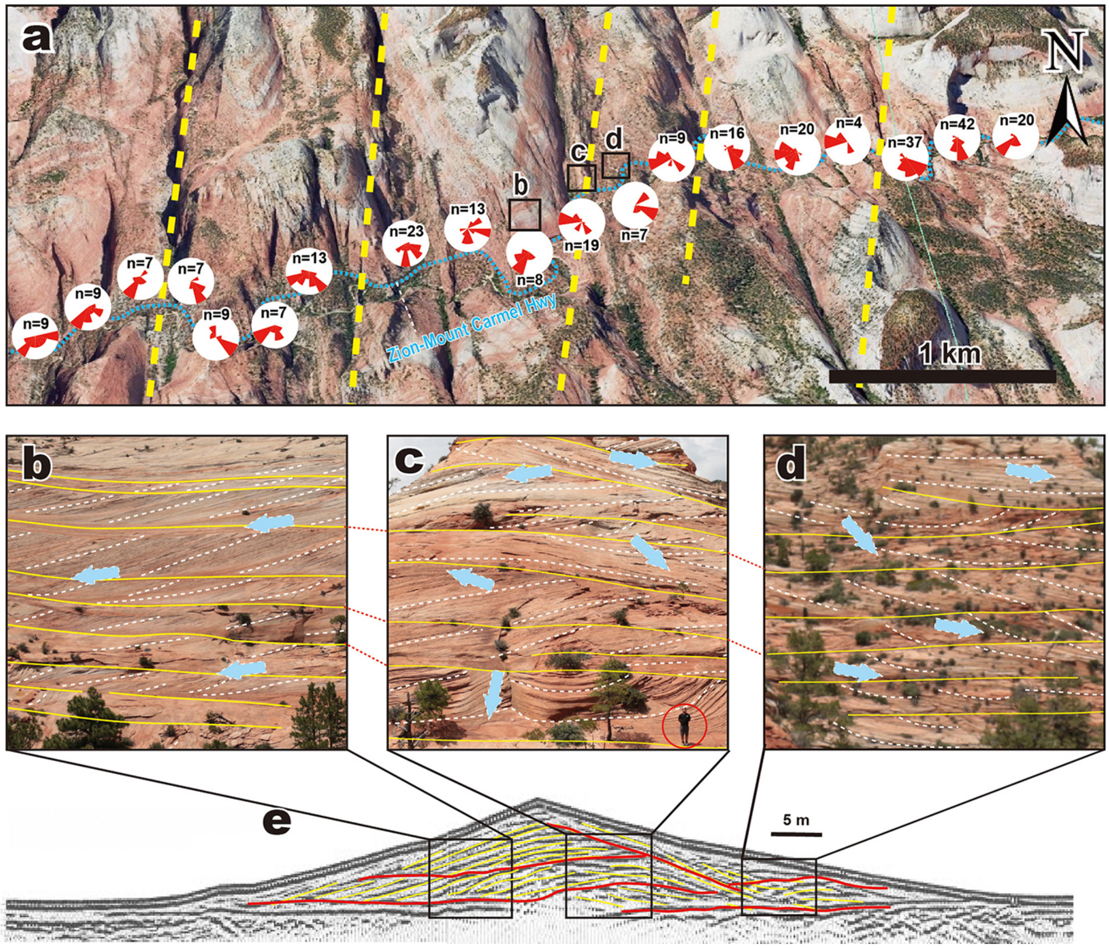

Figure 2. Spatial pattern of dune slip-face azimuths and outcrop photographs of the Navajo Sandstone in the Zion National Park, and comparison with the internal structure of a modern longitudinal dune. **(a)** Spatial distribution of palaeowind data along the Zion–Mount Carmel Highway. Yellow dotted lines are the inferred locations of the central crests of longitudinal dunes, which are spaced at horizontal intervals of ∼ 1 km (© Google Earth 2016). **(b–d)** Outcrop photographs of cross-stratification in the Navajo Sandstone. Yellow solid lines and white dashed lines indicate the bounding surfaces of aeolian dune strata and slip-face cross-stratifications, respectively. All photographs were taken facing north. Red circle in **(c)** indicates a person for scale (ca. 1.7 m tall). **(e)** Ground-penetrating radar (GPR) profiles showing the internal structure of a modern longitudinal dune (Bristow et al., 2000). Yellow and red traces indicate slip faces and unconformities, respectively.

(Bristow et al., 2000, 2007; Zhou et al., 2012; Telfer and Hesse, 2013; Liu and Baas, 2020) (Figs. 2e and 3e). Internally, modern longitudinal dunes exhibit oblique bidirectional cross-beds on each side of the dune flank and stacking of cross-beds in both directions in the central part. In the central parts of longitudinal dunes, the vertical stacking of two oblique opposing-direction cross-sets results in increasing dune height and sets of trough cross-stratification (Figs. 2e and 3e). Optically stimulated luminescence (OSL) dating has further constrained the timing and duration of cross-beds and wind regimes during the formation of cross-bedding (Bristow et al., 2000, 2007; Zhou et al., 2012). Sets of trough cross-stratification are formed in the central dune crest by the superposition of bimodal dunes. These structural features are also observed in outcrops of Navajo Sandstone strata in the Zion and Arches regions (Figs. 2c and 3c), and are therefore interpreted to have been formed by the vertical stacking of cross-sets of longitudinal dunes. The change in preferred direction at horizontal intervals of 1–2 km (Figs. 2a and 3a) is also consistent with the spacing of modern longitudinal dunes (Wasson and Hyde, 1983; Lancaster, 2006).

The angles between the observed bimodal directions of the slip-face azimuth are in good agreement with experimental estimates of the angles between the flow directions that form longitudinal dunes. Water flume experiments simulating the formation of different types of dunes have suggested that longitudinal dunes form under bidirectional flows with angles of 90–135° between flows and lie along the average wind direction (Taniguchi et al., 2012). The formation of longitudinal dunes by seasonal alternations of oblique wind flow

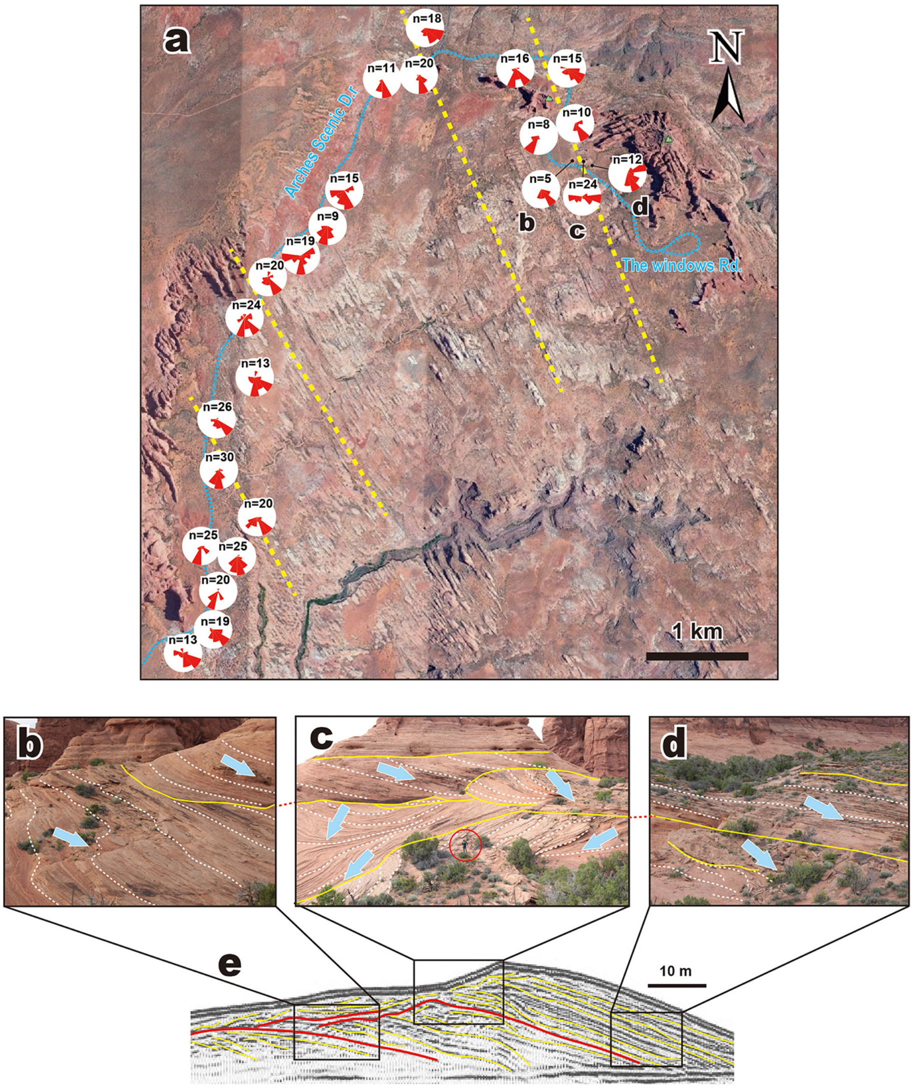

Figure 3. Spatial pattern of dune slip-face azimuths and outcrop photographs of the Navajo Sandstone in the Arches National Park, and comparison with the internal structure of a modern longitudinal dune. **(a)** Spatial distribution of palaeowind data along the Arches Scenic Drive. Yellow dotted lines are the inferred locations of the central crests of longitudinal dunes (© Google Earth 2016). **(b–d)** Outcrop photographs of cross-stratification structures in the Navajo Sandstone. Yellow solid lines and white dashed lines indicate bounding surface and slip-face cross-stratifications, respectively. All photographs were taken facing north. Red circle in **(c)** indicates a person for scale (ca. 1.7 m tall). **(e)** Ground-penetrating radar (GPR) profile showing the internal structure of a modern longitudinal dune (Bristow et al., 2000). Yellow and red traces indicate slip faces and unconformities, respectively.

is also consistent with numerical modelling (Parteli et al., 2014; Gao et al., 2015; Liu and Baas, 2020) and observational studies (Breed et al., 1979; Wasson et al., 1988; Livingstone, 1989; Hesse, 2010; Zhou et al., 2012). It should be noted that longitudinal dunes are also formed under unimodal wind regimes under the influence of vegetation, clay and salt content and related sediment cohesiveness, whilst sinuous unidirectional dunes also form under bimodal wind regimes under the influence of sand availability (du Pont et al., 2014; Gao et al., 2015). However, the zigzag patterns and compound sets of cross-stratification preserved in the Navajo Sandstone in the Zion and Arches regions (Figs. 2c and 3c) resemble the features of longitudinal dunes in other aeolian dune strata (Scherer, 2000; Abrantes et al., 2020). In addition, GPR observations of modern sinuous unidirectional dunes (Fu et al., 2019) indicate bidirectional but relatively thin cross-bed structures compared with those of longitudinal dunes (Bristow et al., 2000, 2007; Zhou et al., 2012; Telfer and Hesse, 2013; Liu and Baas, 2020). Therefore, the Navajo Sandstone in the Zion and Arches regions is interpreted as having been formed by longitudinal dunes, consistent with an earlier suggestion by Rubin and Hunter (1985).

In addition to the outcrop evidence in the Zion and Arches regions, the spatial pattern of slip-face directions suggests that longitudinal dunes were widely distributed in the western US and were oriented NNW–SSE to NNE–SSW in the palaeolatitude range ~ 20–26° N during the Early Jurassic (Fig. 1b). The data further indicate the characteristic wind flow regime in four areas. Specifically, the slip-face azimuths in the southernmost area (palaeolatitude: $\sim 19°$ N) show a bidirectional pattern of eastward and southward palaeowinds, whereas the southwestern and southeastern areas (palaeolatitude: ~ 20–22° N) show preferred SW-ward and SE-ward directions, with a stronger influence of easterly palaeowinds in the southwestern area. The central area (palaeolatitude: $\sim 22°$ N) shows more complex and multidirectional patterns, suggesting the presence of star dunes (Lancaster, 1989). In contrast, the southern part of the northern area (palaeolatitude: $\sim 23°$ N) shows unidirectional SW-ward directions, suggesting the dominance of transverse dunes, which is also consistent with the evidence of NW–SE-oriented underground dune structures inferred from seismic inversion (Verma et al., 2018). The northern area (palaeolatitude: ~ 24–26° N) shows a bidirectional palaeowind pattern toward the SW and SE, whereas the northernmost area (palaeolatitude: $\sim 27°$ N) shows a stronger influence of eastward palaeowind, although the possibility of sampling bias should be considered.

3.2 Comparison of modelled and observed surface wind patterns

The observed tridirectional pattern of slip-face azimuths suggests that the longitudinal dunes were formed as the result of a combination of westerly, northwesterly, and northeasterly palaeowinds (Fig. 1b). The reconstructed trimodal palaeowind directions are consistent with the model-generated prevailing surface wind patterns, including northeasterly trade winds over the study area during the boreal winter and northwesterly winds during the boreal summer (Rowe et al., 2007).

The reconstructed trimodal palaeowind directions are also consistent with model results inferring seasonal- and orbital-scale changes in wind regime (Winguth and Winguth, 2013). The main result of orbitally induced changes in the atmospheric pressure pattern is the predominance of a subtropical low-pressure system (continental) at ~ 20–25° N in the boreal summer during the eccentricity-modulated precession maximum (Winguth and Winguth, 2013; Fig. 4c). The resulting large subtropical low-pressure cell diverts the moist tropical air masses of the ITCZ away from Panthalassa and results in strong precipitation across subtropical Pangaea (Winguth and Winguth, 2013). In contrast, the development of the strong continental high-pressure system at $\sim 30°$ N results in the dominance of dry NE trade winds over the study area during winter (Winguth and Winguth, 2013; Fig. 4a). The movement of dune sand was probably stabilized by intense summer rainfall and the resulting higher groundwater table and enhanced vegetation (Kocurek, 2003; Durán and Herrmann, 2006; Hesse and Simpson, 2006), which seems consistent with the development of bounding surfaces and evidence of trace fossils (invertebrate burrows) within dune slip faces in south-central Utah (Chan and Archer, 2000; Loope and Rowe, 2003; Ekdale et al., 2007).

On the other hand, the development of a high-pressure system led to arid climatic conditions over the entire study area in both summer and winter during the eccentricity-modulated precession minimum (Winguth and Winguth, 2013; Fig. 4b and d). The boreal summer precipitation was reduced in subtropical Pangaea, and the strengthening of the high-pressure system over the Panthalassa resulted in dry NW and NNW winds (Winguth and Winguth, 2013). In addition, the continental high-pressure system (weaker than the insolation maximum) resulted in dry NE trade winds during the boreal winter (Winguth and Winguth, 2013). Because of this seasonal and orbital-scale wind regime alternation between the eccentricity-modulated precession maximum (winter: NE trade winds; summer: dune stabilization) and minimum (winter: NE trade winds; summer: NW and NNW winds), NNE–SSW- to NNW–SSE-oriented longitudinal dunes are inferred to have formed in the southern and central areas (~ 20–25° N) (Fig. 4). In the northernmost area ($\sim 27°$ N), westerly winds dominated in summer during the eccentricity-modulated precession minimum, forming eastward-migrating transverse dunes (Fig. 4b).

Previous studies also raised the possibility that orbital-scale climatic changes are recorded in aeolian depositional sequences in subtropical Pangaea, such as fluvial–aeolian cycles (~ 20 m thick) in the Lower Jurassic Navajo–Kayenta transition in Utah (Hassan et al., 2018), aeolian cyclic sequences (~ 4–8 and ~ 18–22 m thick) in the Permian Cedar Mesa Sandstone in Utah (Mountney, 2006), and aeolian–alluvial cycles (~ 2–15 m thick) in the Permian Ingleside Formation in Colorado (Pike and Sweet, 2018), which are interpreted as reflecting the 100 and 400 kyr eccentricity cycles. A previous study also suggested that the bioturbated zones and the bounding surfaces in the Navajo Sandstone likely reflected orbital-scale pluvial episodes (Loope and Rowe, 2003). Although the Navajo Sandstone in the Zion region does not contain well-defined facies cycles or well-developed palaeosols, the bounding surfaces appear to occur every ca. 2.9 ± 0.9 m of stratigraphic thickness (Fig. 2b–d; see the table in the Supplement). On the basis of existing chronological data (Dickinson and Gehrels, 2009; Dickinson et al., 2010), we estimated the duration of deposition of the Navajo Sandstone to be ca. 14.7–19.4 Myr and its thickness to be 300–700 m; thus, the average accumulation rate can be calculated as ca. 1.5–4.8 cm kyr^{-1}. Based on this estimated accumulation rate, the bounding surfaces of dune strata (every ~ 2.9 m) likely formed at intervals of 60–193 kyr, which is in agreement with the timescale of the 100 kyr eccentricity cycle, consistent with previous studies, although further

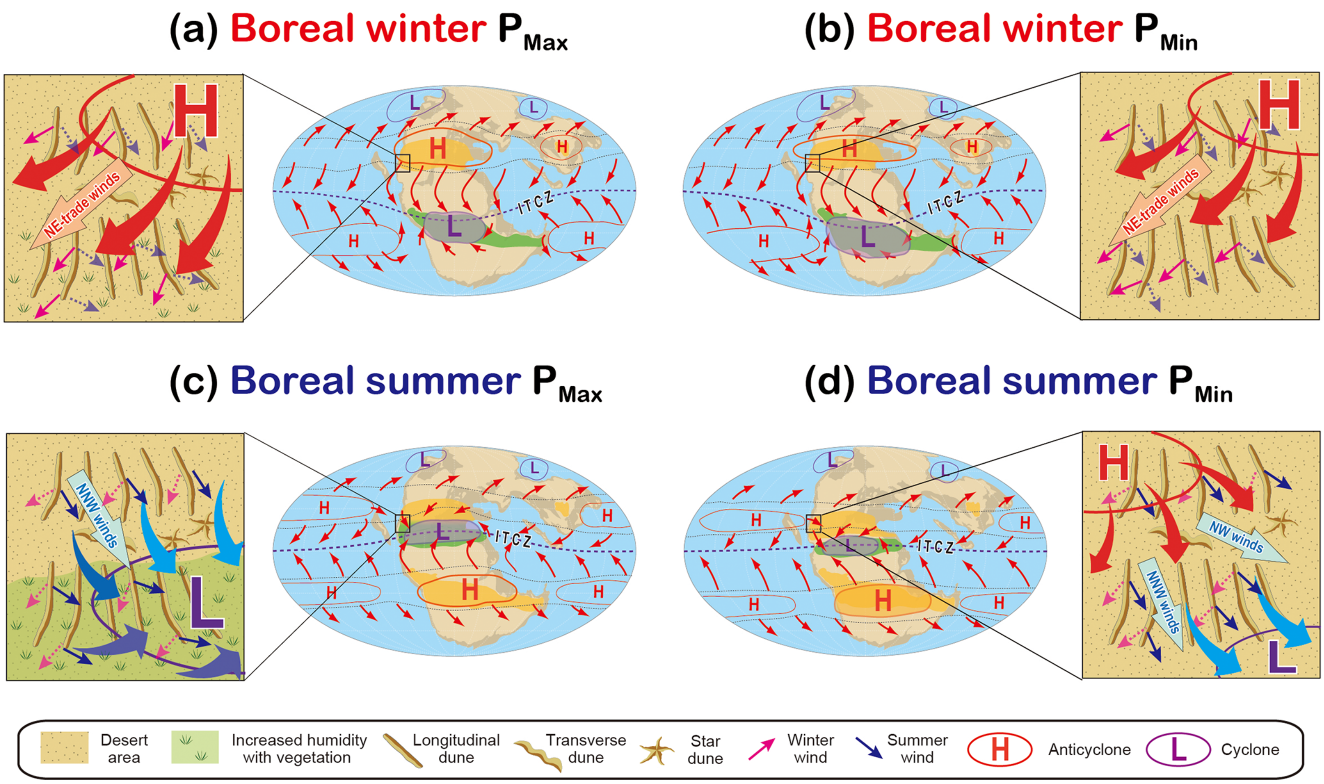

Figure 4. Schematic illustrations of orbital and seasonal changes in the Pangaean atmospheric pressure pattern and inferred dune alignments in the western US during the eccentricity-modulated precession maximum (P_{Max}; **a, c**) and minimum (P_{Min}; **b, d**). Orbital-scale changes in the pressure pattern are based on climatic model results (Winguth and Winguth, 2013). Seasonal changes in wind regimes are indicated as pink (boreal winter) and blue (boreal summer) arrows. During the eccentricity-modulated precession maximum, the continental low-pressure system in the boreal summer was likely reduced by a few hPa relative to the eccentricity-modulated precession minimum in response to the increase in surface temperature (Winguth and Winguth, 2013). Increased moisture and vegetation cover likely resulted in dune stabilization in the southern area during the boreal summer at the eccentricity-modulated precession maximum **(c)**.

chronological and sedimentological studies are required to test this hypothesis.

These lines of evidence, in conjunction with a comparison of observed palaeowind directions and model-generated wind patterns, indicate that orbital-scale climate change may have influenced the development of longitudinal dune fields in Pangaea. Although preservation of the palaeoenvironmental record is generally hampered by the erosion of aeolian deposits, it is likely that the Navajo Sandstone was deposited with a higher rate of sand supply than that of the present-day Sahara Desert (Kocurek, 2003), which may have enabled the preservation of orbital-scale palaeoclimatic records. Nevertheless, the formation mechanisms of bounding surfaces and their responses to orbital-scale climatic changes remain uncertain even in the Quaternary, due to the stochastic noise from deposition/erosion and sampling issues (e.g. Hesse, 2016; Leighton et al., 2014; Telfer et al., 2010; Thomas and Bailey, 2017). Thus, further investigation is required to test our hypothesis.

4 Conclusions

A comparison of climate model reconstructions with dune slip-face azimuth data indicates that Lower Jurassic longitudinal dunes in the western US likely reflect seasonal- and orbital-scale changes in the wind regime and atmospheric pressure pattern over Pangaea. Revised palaeomagnetic data and palaeowind data of the present study do not support desert development and predominant westerly winds in equatorial Pangaea during the Early Jurassic, in contrast to the results of Loope et al. (2004). NNE–SSW- to NNW–SSE-oriented longitudinal dunes in the central and southern parts of the study area and eastward-migrating unidirectional dunes in the northernmost parts are interpreted to have formed as the result of superimposed seasonal and orbital changes in wind regimes. The reconstructed palaeowind pattern at $\sim$ 19–27° N appears to be consistent with model-generated surface wind patterns and the location of the subtropical high-pressure belt. Therefore, we have solved the enigma of Pangaean atmospheric circulation patterns, such as the discrepancy between model-generated wind directions and aeolian dune records as noted by Rowe et al. (2007). The results also indicate the influence of orbitally induced climate change on longitudinal dune development in subtropical Pangaea, although further chronological and sedimentological studies are required to test this hypothesis.

Data availability. All datasets are shown in the Supplement.

Supplement. The supplement related to this article is available online at: https://doi.org/10.5194/cp-18-1529-2022-supplement.

Author contributions. HH designed this research. HS and HH conducted the field survey and wrote the manuscript.

Competing interests. The contact author has declared that neither they nor their co-authors have any competing interests.

Disclaimer. Publisher's note: Copernicus Publications remains neutral with regard to jurisdictional claims in published maps and institutional affiliations.

Acknowledgements. We greatly appreciate Hirofumi Asahi for his assistance with the statistical analysis of palaeowind direction data using the EM algorithm from the MATLAB software. We also thank Masayuki Ikeda and Ryusei Kuma for discussions and field assistance. We are also grateful to the editor Zhengtang Guo, Yongyun Hu, and an anonymous reviewer for their constructive comments.

Review statement. This paper was edited by Zhengtang Guo and reviewed by Yongyun Hu and one anonymous referee.

References

Abrantes, F. R., Basilici, G., and Soares, M. V. T.: Mesoproterozoic erg and sand sheet system: Architecture and controlling factors (Galho do Miguel Formation, SE Brazil), Precambrian Res., 338, 105592, https://doi.org/10.1016/j.precamres.2019.105592, 2020.

Beveridge, C., Kocurek, G., Ewing, R. C., Lancaster, N., Morthekai, P., Singhvi, A. K., and Mahan, S. A.: Development of spatially diverse and complex dune-field patterns: Gran Desierto Dune Field, Sonora, Mexico, Sedimentology, 53, 1391–1409, https://doi.org/10.1111/j.1365-3091.2006.00814.x, 2006.

Blakey, R. C.: Pennsylvanian-Jurassic Sedimentary Basins of the Colorado Plateau and Southern Rocky Mountains, in: The Sedimentary Basins of the United States and Canada, edited by: Miall, A. D., Elsevier, 245–296, https://doi.org/10.1016/S1874-5997(08)00007-5, 2008.

Blakey, R. C., Peterson, F., and Kocurek, G.: Synthesis of late Paleozoic and Mesozoic eolian deposits of the Western Interior of the United States, Sediment. Geol., 56, 3–125, https://doi.org/10.1016/0037-0738(88)90050-4, 1988.

Breed, C. S., Fryberger, S. G., Andrews, S., McCauley, C., Lennartz, F., Geber, D. and Horstman, K.: Regional studies of sand seas using LANDSAT (ERTS) imagery, in: A Study of Global Sand Seas, edited by: McKee, E. D., US Government Printing Office, 305–397, https://doi.org/10.3133/pp1052, 1979.

Bristow, C. S., Balley, S. D., and Lancaster, N.: The sedimentary structure of linear sand dunes, Nature, 406, 56–59, https://doi.org/10.1038/35017536, 2000.

Bristow, C. S., Duller, G. A. T., and Lancaster, N.: Age and dynamics of linear dunes in the Namib Desert, Geology, 35, 555–558, https://doi.org/10.1130/G23369A.1, 2007.

Chan, M. A. and Archer, A. W.: Cyclic Eolian Stratification on the Jurassic Navajo Sandstone, Zion National Park: Periodicities and Implications for Paleoclimate, in: Geology of Utah's Parks and Monuments, edited by: Sprinkel, D. A., Anderson, P. B., and Chidsey, T. C., Utah Geological Association Publication., 607–617, ISBN 9781882054107, 2000.

Dickinson, W. R.: Tectonosedimentary relations of Pennsylvanian to Jurassic Strata on the Colorado Plateau, Spec. Pap. Geol. Soc. Am., 533, 1–184, https://doi.org/10.1130/2018.2533, 2018.

Dickinson, W. R. and Gehrels, G. E.: Use of U–Pb ages of detrital zircons to infer maximum depositional ages of strata: A test against a Colorado Plateau Mesozoic database, Earth Planet. Sci. Lett., 288, 115–125, https://doi.org/10.1016/j.epsl.2009.09.013, 2009.

Dickinson, W. R., Stair, K. N., Gehrels, G. E., Peters, L., Kowallis, B. J., Blakey, R. C., Amar, J. R., and Greenhalgh, B. W.: Geological note: U–Pb and ^{40}Ar/^{39}Ar ages for a tephra lens in the middle jurassic page sandstone: First direct isotopic dating of a mesozoic eolianite on the colorado plateau, J. Geol., 118, 215–221, https://doi.org/10.1086/649819, 2010.

du Pont, S. C., Narteau, C., and Gao, X.: Two modes for dune orientation, Geology, 42, 743–746, https://doi.org/10.1130/G35657.1, 2014.

Durán, O. and Herrmann, H. J.: Vegetation against dune mobility, Phys. Rev. Lett., 97, 1–4, https://doi.org/10.1103/PhysRevLett.97.188001, 2006.

Ekdale, A. A., Bromley, R. G. and Loope, D. B.: Ichnofacies of an Ancient Erg: A Climatically Influenced Trace Fossil Association in the Jurassic Navajo Sandstone, Southern Utah, USA, in: Trace Fossils: Concepts, Problems, Prospects, edited by: Miller, W., Elsevier, 562–574, https://doi.org/10.1016/B978-044452949-7/50161-3, 2007.

Fu, T., Wu, Y., Tan, L., Li, D., and Wen, Y.: Imaging the structure and reconstructing the development of a barchan dune using ground-penetrating radar, Geomorphology, 341, 192–202, https://doi.org/10.1016/j.geomorph.2019.05.014, 2019.

Gao, X., Narteau, C., Rozier, O., and Du Pont, S. C.: Phase diagrams of dune shape and orientation depending on sand availability, Sci. Rep., 5, 1–12, https://doi.org/10.1038/srep14677, 2015.

Hasegawa, H., Tada, R., Jiang, X., Suganuma, Y., Imsamut, S., Charusiri, P., Ichinnorov, N., and Khand, Y.: Drastic shrinking of the Hadley circulation during the mid-Cretaceous Supergreenhouse, Clim. Past, 8, 1323–1337, https://doi.org/10.5194/cp-8-1323-2012, 2012.

Hassan, M. S., Venetikidis, A., Bryant, G., and Miall, A. D.: The sedimentology of an erg margin: The kayenta-navajo transition (lower jurassic), kanab, Utah, USA, J. Sediment. Res., 88, 613–640, https://doi.org/10.2110/jsr.2018.31, 2018.

Hesse, P. P.: The Australian desert dunefields: Formation and evolution in an old, flat, dry continent, Geol. Soc. Spec. Publ., 346, 141–164, https://doi.org/10.1144/SP346.9, 2010.

Hesse, P. P.: How do longitudinal dunes respond to climate forcing? Insights from 25 years of luminescence dating of the Australian desert dunefields, Quat. Int., 410, 11–29, https://doi.org/10.1016/j.quaint.2014.02.020, 2016.

Hesse, P. P. and Simpson, R. L.: Variable vegetation cover and episodic sand movement on longitudinal desert sand dunes, Geomorphology, 81, 276–291, https://doi.org/10.1016/j.geomorph.2006.04.012, 2006.

Kent, D. V. and Irving, E.: Influence of inclination error in sedimentary rocks on the Triassic and Jurassic apparent pole wander path for North America and implications for Cordilleran tectonics, J. Geophys. Res. Solid Earth, 115, 1–25, https://doi.org/10.1029/2009JB007205, 2010.

Kocurek, G.: Interpretation of Ancient Eolian Sand Dunes, Annu. Rev. Earth Planet. Sci., 19, 43–75, https://doi.org/10.1146/annurev.ea.19.050191.000355, 1991.

Kocurek, G.: Limits on extreme eolian systems: Sahara of Mauritania and Jurassic Navajo Sandstone examples, Spec. Pap. Geol. Soc. Am., 370, 43–52, https://doi.org/10.1130/0-8137-2370-1.43, 2003.

Kutzbach, J. E.: Idealized Pangean climates: Sensitivity to orbital change, in: Paleoclimate, Tectonism, and Sedimentation during Accretion, Zenith, and Breakup of a Supercontinent, edited by: Klein, G. O., Geological Society of America Special Papers, 41–55, https://doi.org/10.1130/SPE288-p41, 1994.

Kutzbach, J. E. and Gallimore, R. G.: Pangaean climates: megamonsoons of the megacontinent, J. Geophys. Res., 94, 3341–3357, https://doi.org/10.1029/JD094iD03p03341, 1989.

Lancaster, N.: Paleoenvironmental implications of fixed dune systems in Southern Africa, Palaeogeogr. Palaeoclimatol. Palaeoecol., 33, 327–346, https://doi.org/10.1016/0031-0182(81)90025-0, 1981.

Lancaster, N.: Star Dunes, Prog. Phys. Geogr., 13, 67–91, https://doi.org/10.1177/030913338901300105, 1989.

Lancaster, N.: Palaeoclimatic evidence from sand seas, Palaeogeogr. Palaeoclimatol. Palaeoecol., 76, 279–290, https://doi.org/10.1016/0031-0182(90)90116-O, 1990.

Lancaster, N.: Linear Dunes on Titan, Science, 312, 702–703, https://doi.org/10.1126/science.1126292, 2006.

Lancaster, N., Kocurek, G., Singhvi, A., Pandey, V., Deynoux, M., Ghienne, J.-F., and Lô, K.: Late Pleistocene and Holocene dune activity and wind regimes in the western Sahara Desert of Mauritania, Geology, 30, 991, https://doi.org/10.1130/0091-7613(2002)030<0991:LPAHDA>2.0.CO;2, 2002.

Leighton, C. L., Bailey, R. M., and Thomas, D. S. G.: Interpreting and modelling late Quaternary dune accumulation in the southern Arabian Peninsula, Quat. Sci. Rev., 102, 1–13, https://doi.org/10.1016/j.quascirev.2014.08.002, 2014.

Liu, Y. and Baas, A. C. W.: Internal sedimentary structure of linear dunes modelled with a cellular automaton, Sedimentology, 67, 3718–3734, https://doi.org/10.1111/sed.12767, 2020.

Livingstone, I.: Monitoring surface change on a Namib linear dune, Earth Surf. Process. Landforms, 14, 317–332, https://doi.org/10.1002/esp.3290140407, 1989.

Loope, D. B. and Rowe, C. M.: Long-Lived Pluvial Episodes during Deposition of the Navajo Sandstone, J. Geol., 111, 223–232, https://doi.org/10.1086/345843, 2003.

Loope, D. B., Steiner, M. B., Rowe, C. M., and Lancaster, N.: Tropical westerlies over Pangaean sand seas, Sedimentology, 51, 315–322, https://doi.org/10.1046/j.1365-3091.2003.00623.x, 2004.

Marzolf, J. E.: Controls on late Paleozoic and early Mesozoic eolian deposition of the western United States, Sediment. Geol., 56, 167–191, https://doi.org/10.1016/0037-0738(88)90053-X, 1988.

Mountney, N. P.: Periodic accumulation and destruction of aeolian erg sequences in the Permian Cedar Mesa Sandstone, White Canyon, southern Utah, USA, Sedimentology, 53, 789–823, https://doi.org/10.1111/j.1365-3091.2006.00793.x, 2006.

Parrish, J. T.: Climate of the Supercontinent Pangea, J. Geol., 101, 215–233, https://doi.org/10.1086/648217, 1993.

Parrish, J. T. and Peterson, F.: Wind directions predicted from global circulation models and wind directions determined from eolian sandstones of the western United States – A comparison, Sediment. Geol., 56, 261–282, https://doi.org/10.1016/0037-0738(88)90056-5, 1988.

Parrish, J. T., Rasbury, E. T., Chan, M. A., and Hasiotis, S. T.: Earliest Jurassic U–Pb ages from carbonate deposits in the Navajo Sandstone, southeastern Utah, USA, Geology, 47, 1015–1019, https://doi.org/10.1130/G46338.1, 2019.

Parteli, E. J. R., Kroy, K., Tsoar, H., Andrade, J. S., and Pöschel, T.: Morphodynamic modeling of aeolian dunes: Review and future plans, Eur. Phys. J. Spec. Top., 223, 2269–2283, https://doi.org/10.1140/epjst/e2014-02263-2, 2014.

Peterson, F.: Pennsylvanian to Jurassic eolian transportation systems in the western United States, Sediment. Geol., 56, 207–260, https://doi.org/10.1016/0037-0738(88)90055-3, 1988.

Pike, J. D. and Sweet, D. E.: Environmental drivers of cyclicity recorded in lower Permian eolian strata, Manitou Springs, Colorado, western United States, Palaeogeogr. Palaeoclimatol. Palaeoecol., 499, 1–12, https://doi.org/10.1016/j.palaeo.2018.03.026, 2018.

Rodríguez-López, J. P., Melendez, N., De Boer, P. L., and Soria, A. R.: Aeolian sand sea development along the mid-Cretaceous western Tethyan margin (Spain): erg sedimentology and palaeoclimate implications, Sedimentology, 55, 1253–1292, doi.org/10.1111/j.1365-3091.2007.00945.x, 2008.

Rowe, C. M., Loope, D. B., Oglesby, R. J., Van Der Voo, R., and Broadwater, C. E.: Inconsistencies between Pangean reconstructions and basic climate controls, Science, 318, 1284–1286, https://doi.org/10.1126/science.1146639, 2007.

Rowland, S. M. and Mercadante, J. M.: Trackways of a gregarious, dunefield-dwelling, Early Jurassic therapsid in the Aztec Sandstone of southern Nevada, Palaios, 29, 539–552, https://doi.org/10.2110/palo.2013.067, 2014.

Rubin, D. M. and Hunter, R. E.: Why deposits of longitudinal dunes are rarely recognized in the geologic record, Sedimentology, 32, 147–157, https://doi.org/10.1111/j.1365-3091.1985.tb00498.x, 1985.

Scherer, C. M. S.: Eolian dunes of the Botucatu Formation (Cretaceous) in southernmost Brazil: Morphology and origin, Sediment. Geol., 137, 63–84, https://doi.org/10.1016/S0037-0738(00)00135-4, 2000.

Sprinkel, D. A., Kowallis, B. J., and Jensen, P. H.: Correlation and Age of the Nugget Sandstone and Glen Canyon Group, Utah, in: Sevier thrust belt: Northern and central Utah and adjacent areas, edited by: Sprinkel, D. A., Yonkee, W. A., and Chidsey, T. C., Geological Association, Salt Lake City, Utah, 131–149, ISBN 9780980048933, 2011.

Sridhar, V., Loope, D. B., Swinehart, J. B., Mason, J. A., Oglesby, R. J., and Rowe, C. M.: Large Wind Shift on the Great Plains During the Medieval Warm Period, Science, 313, 345–347, https://doi.org/10.1126/science.1128941, 2006.

Taniguchi, K., Endo, N., and Sekiguchi, H.: The effect of periodic changes in wind direction on the deformation and morphology of isolated sand dunes based on flume experiments and field data from the Western Sahara, Geomorphology, 179, 286–299, https://doi.org/10.1016/j.geomorph.2012.08.019, 2012.

Tape, C.: The Lower Jurassic Navajo Sandstone: large-scale deposition and small-scale structures, Guidebook of Field Trip to Colorado Plateau (southern Utah, northern Arizona, Permian-Triassic boundary), Natural History Museum of Utah, 11 pp., https://nhmu.utah.edu/sites/default/files/trail-resource/Navajo%20Sandstone.pdf (last access: 5 July 2022), 2005.

Telfer, M. W. and Hesse, P. P.: Palaeoenvironmental reconstructions from linear dunefields: Recent progress, current challenges and future directions, Quat. Sci. Rev., 78, 1–21, https://doi.org/10.1016/j.quascirev.2013.07.007, 2013.

Telfer, M. W., Bailey, R. M., Burrough, S. L., Stone, A. E. S., Thomas, D. S. G., and Wiggs, G. S. F.: Understanding linear dune chronologies: Insights from a simple accumulation model, Geomorphology, 120, 195–208, https://doi.org/10.1016/j.geomorph.2010.03.030, 2010.

Thébault, E., Finlay, C. C., Beggan, C. D., Alken, P., Aubert, J., Barrois, O., Bertrand, F., Bondar, T., Boness, A., Brocco, L., Canet, E., Chambodut, A., Chulliat, A., Coïsson, P., Civet, F., Du, A., Fournier, A., Fratter, I., Gillet, N., Hamilton, B., Hamoudi, M., Hulot, G., Jager, T., Korte, M., Kuang, W., Lalanne, X., Langlais, B., Léger, J.-M., Lesur, V., Lowes, F. J., Macmillan, S., Mandea, M., Manoj, C., Maus, S., Olsen, N., Petrov, V., Ridley, V., Rother, M., Sabaka, T. J., Saturnino, D., Schachtschneider, R., Sirol, O., Tangborn, A., Thomson, A., Tøffner-Clausen, L., Vigneron, P., Wardinski, I., and Zvereva, T.: International Geomagnetic Reference Field: the 12th generation, Earth Planets Sp., 67, 79, https://doi.org/10.1186/s40623-015-0228-9, 2015.

Thomas, D. S. G. and Bailey, R. M.: Is there evidence for global-scale forcing of Southern Hemisphere Quaternary desert dune accumulation? A quantitative method for testing hypotheses of dune system development, Earth Surf. Process. Landforms, 42, 2280–2294, https://doi.org/10.1002/esp.4183, 2017.

Tomita, S. and Yamaji, A.: KUT: Software to Rotate Orientation Data, Geoinformatics, 14, 85–104, https://doi.org/10.6010/geoinformatics.14.85, 2003.

Verma, S., Bhattacharya, S., Lujan, B., Agrawal, D., and Mallick, S.: Delineation of early Jurassic aged sand dunes and paleo-wind direction in southwestern Wyoming using seismic attributes, inversion, and petrophysical modeling, J. Nat. Gas Sci. Eng., 60, 1–10, https://doi.org/10.1016/j.jngse.2018.09.022, 2018.

Wasson, R. J. and Hyde, R.: Factors determining desert dune type, Nature, 304, 337–339, https://doi.org/10.1038/304337a0, 1983.

Wasson, R. J., Fitchett, K., Mackey, B., and Hyde, R.: Large-scale patterns of dune type, spacing and orientation in the australian continental dunefield, Aust. Geogr., 19, 89–104, https://doi.org/10.1080/00049188808702952, 1988.

Winguth, A. and Winguth, C.: Precession-driven monsoon variability at the Permian-Triassic boundary – Implications for anoxia and the mass extinction, Glob. Planet. Change, 105, 160–170, https://doi.org/10.1016/j.gloplacha.2012.06.006, 2013.

Zhou, J., Zhu, Y., and Yuan, C.: Origin and lateral migration of linear dunes in the Qaidam Basin of NW China revealed by dune sediments, internal structures, and optically stimulated luminescence ages, with implications for linear dunes on Titan, Bull. Geol. Soc. Am., 124, 1147–1154, https://doi.org/10.1130/B30550.1, 2012.